ChemPubSoc Europe

FULL PAPERS

Ambidexterity! The compounds reported herein were characterized as inhibitors of anti-apoptotic Bcl-2 family proteins. Structures in this compound class contain a chiral center (C4 atom) on the pyrimidine ring. Interestingly, our study revealed that the *R* and *S* enantiomers of this compound class have similar binding affinities for Bcl-x_L, Bcl-2, and Mcl-1.

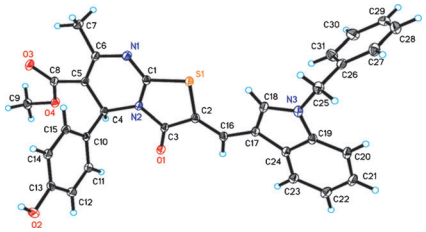

Y. Xu, M. Zhou, Y. Li, C. Li, Z. Zhang, B. Yu, R. Wang**

■■ – ■■

Characterization of the Stereochemical Structures of 2*H*-Thiazolo[3,2-*a*]pyrimidine Compounds and Their Binding Affinities for Anti-apoptotic Bcl-2 Family Proteins

DOI: 10.1002/cmdc.201300159

Characterization of the Stereochemical Structures of 2*H*-Thiazolo[3,2-*a*]pyrimidine Compounds and Their Binding Affinities for Anti-apoptotic Bcl-2 Family Proteins

Yaochun Xu, Mi Zhou, Yan Li, Chengke Li, Zhengxi Zhang, Biao Yu,* and Renxiao Wang*[a]

In a previous study we reported a class of compounds with a 2*H*-thiazolo[3,2-*a*]pyrimidine core structure as general inhibitors of anti-apoptotic Bcl-2 family proteins. However, the absolute stereochemical configuration of one carbon atom on the core structure remained unsolved, and its potential impact on the binding affinities of compounds in this class was unknown. In this study, we obtained pure *R* and *S* enantiomers of four selected compounds by HPLC separation and chiral synthesis. The absolute configurations of these enantiomers were determined by comparing their circular dichroism spectra to that of an appropriate reference compound. In addition, a crystal structure of one selected compound revealed the exocyclic double bond in these compounds to be in the *Z* configuration. The binding affinities of all four pairs of enantiomers to Bcl-x_L, Bcl-2, and Mcl-1 proteins were measured in a fluorescence-polarization-based binding assay, yielding inhibition constants (K_i values) ranging from 0.24 to 2.20 μM. Interestingly, our results indicate that most *R* and *S* enantiomers exhibit similar binding affinities for the three tested proteins. A binding mode for this compound class was derived by molecular docking and molecular dynamics simulations to provide a reasonable interpretation of this observation.

Introduction

As key regulators of apoptosis (programmed cell death), Bcl-2 family proteins have drawn much attention since the late 1990s.[1–3] Anti-apoptotic members of this family such as Bcl-2, Bcl-x_L, and Mcl-1 bind and sequester pro-apoptotic members such as Bim, Puma, Noxa, Bad, and Bax, thereby preventing mitochondria-mediated cell death. Various tumor cell types are found to overexpress at least one of these proteins, which provides a mechanism for those cells to resist apoptosis induced by chemotherapy or radiation. Recent studies have revealed that Bcl-2 family proteins also play important roles in other cellular events such as autophagy[4] and cell proliferation.[5] Thus, the development of small-molecule inhibitors targeting anti-apoptotic Bcl-2 family proteins has become a promising approach in the discovery of new anticancer therapies.[6]

Bcl-2 family proteins execute their biological functions through protein–protein interactions. This type of target is normally more difficult to address in drug discovery. Despite the challenge, a range of small-molecule inhibitors of anti-apoptotic Bcl-2 family proteins have been reported thus far.[7–22] Some of them, such as ABT-263,[7,8] gossypol,[9,10] and GX15-070,[11] have already been tested in clinical trials. However, no Bcl-2 inhibitor has been approved yet for entry into the market as an anticancer drug. This situation therefore demands continuous effort toward the discovery of new Bcl-2 inhibitors to eventually reach the goal of an effective anticancer agent.

In our previous study,[23] we reported a class of compounds with a 2*H*-thiazolo[3,2-*a*]pyrimidine core structure as general inhibitors of anti-apoptotic Bcl-2 family proteins (Figure 1). The lead compound was discovered by chance. A series of derivative compounds were then obtained under the guidance of structure-based drug design to improve potency. Indeed, some new compounds exhibited promising binding affinities (K_i < 100 nM). Their specific binding to the target proteins was also confirmed by ^{15}N-HSQC NMR experiments. An advantage of this compound class is that some members are effective binders of Mcl-1 as well as Bcl-x_L or Bcl-2. Such compounds may be

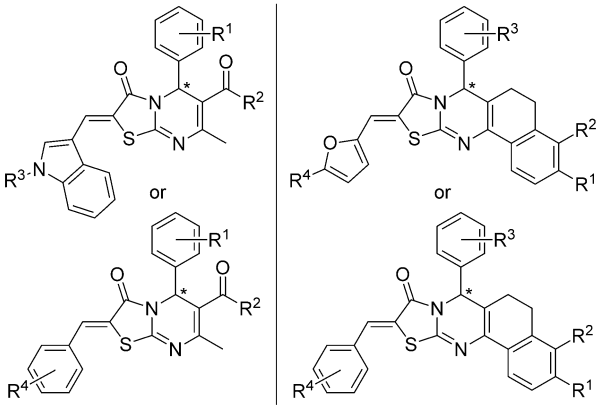

Figure 1. Structures of the compounds previously reported by us (left)[23] and Feng et al. (right).[26]

[a] *Y. Xu, M. Zhou, Y. Li, C. Li, Z. Zhang, Prof. B. Yu, Prof. R. Wang*
State Key Laboratory of Bioorganic and Natural Products Chemistry
Shanghai Institute of Organic Chemistry, Chinese Academy of Sciences
345 Lingling Road, Shanghai 200032 (P.R. China)
E-mail: byu@mail.sioc.ac.cn
wangrx@mail.sioc.ac.cn

Supporting information for this article is available on the WWW under http://dx.doi.org/10.1002/cmdc.201300159.

used for treating cancer cells that resist Bcl-2/Bcl-x_L inhibitors or other chemotherapies through overexpression of Mcl-1.[24,25]

The structure–activity relationships of this class of compounds were described in our previous study.[23] However, the absolute stereochemical configuration of the C4 atom on the core structure remained unsolved. Whether the corresponding *R* and *S* enantiomers elicit different biological effects, as is the case with some other chiral drugs, was also unknown. Feng et al. reported a set of compounds with a core structure similar to ours (Figure 1), which were also characterized as Bcl-2 inhibitors (IC_{50}: 2–70 μM).[26] In their work, enantiomers of one selected compound were separated by chiral HPLC. Subsequent binding assay results indicated that the *R* enantiomer had decent binding affinity (IC_{50} = 1.9 μM), whereas the *S* enantiomer was essentially inactive. However, we were skeptical of their observation, as a predicted binding mode of this compound class derived in our previous study did not quite support it.

The specific aim of this study was to address this issue. We synthesized four compounds of this class and obtained their pure *R* and *S* enantiomers by HPLC separation and chiral synthesis. Their absolute configuration was determined by comparing their circular dichroism (CD) spectra to that of an appropriate reference compound. The crystal structure of one compound was also obtained. All four pairs of enantiomers were tested for their binding affinities to three anti-apoptotic Bcl-2 family proteins in a fluorescence polarization (FP)-based binding assay. Our results indicate that the binding affinities of most pairs of *R* and *S* enantiomers were similar. A binding mode of this compound class was proposed by molecular modeling to interpret this observation.

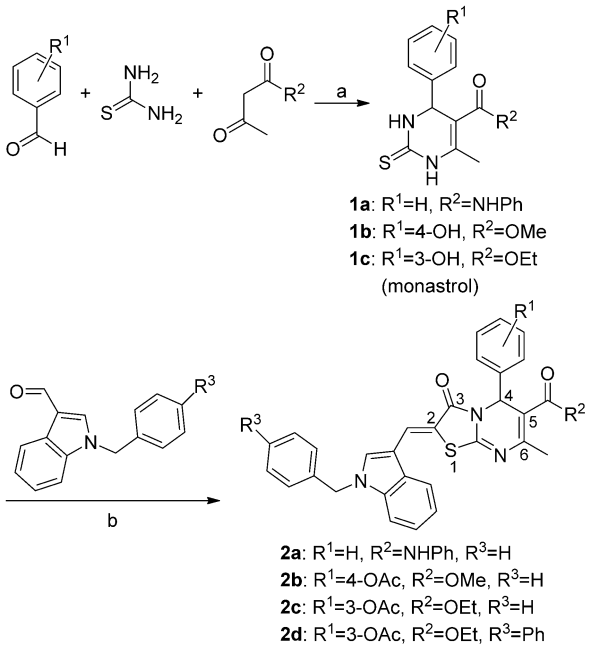

Scheme 1. Synthesis of thiazolo[3,2-*a*]pyrimidinone compounds. *Reagents and conditions*: a) *p*-TsOH, H_2O, EtOH, reflux, 24 h; b) 2-chloroacetic acid, AcOH, Ac_2O, AcONa, 80 °C, 24 h.

Results and Discussion

At the initial attempt, we selected and synthesized two compounds described in our previous study:[23] **2a** (BCL-LZH-02) and **2b** (BCL-LZH-18). The former was the lead compound chosen for optimization in our previous study, and the latter was one of the best compounds obtained by us so far. These two compounds were synthesized by procedures outlined in Scheme 1. The products were then separated by preparative chiral HPLC to obtain pure enantiomers.

We then attempted to resolve the stereochemical structures of these two compounds through crystal structure determination. Growth of single crystals was attempted for two pairs of enantiomers as well as the original racemic mixture. A number of conditions were tested, but unfortunately all trials failed to obtain single crystals of sufficient quality for structure determination. As an additional attempt, **2b** was deacetylated with saturated K_2CO_3 in CH_2Cl_2/CH_3OH (*v*/*v* = 1:1) to obtain a derivative compound with a free hydroxy group on the phenyl ring. Good crystals were obtained from the racemic mixture of this compound and were used in structure determination.

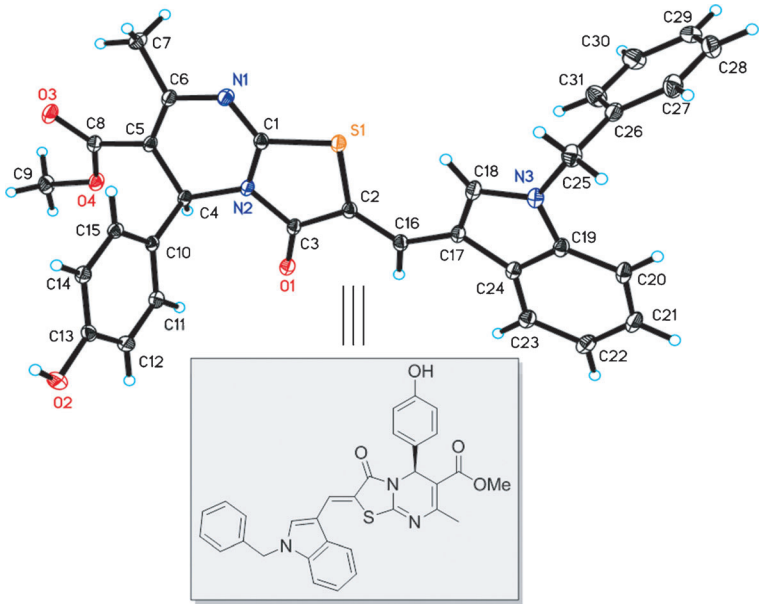

Figure 2. Crystal structure of deacetylated (*S*)-**2b** (CCDC entry 942185).

The resolved crystal structure of deacetylated **2b** is shown in Figure 2. It is evident that the chiral C4 atom is in the *S* configuration in this particular structure. Although this crystal structure did not really help us to determine the absolute configuration of the obtained enantiomers of **2a** or **2b**, it resolved another uncertainty in the stereochemical structure of this class of compounds: The exocyclic double bond connecting the five-membered thiazole ring and the rest of the molecule, that is, C2=C16, is in the *Z* configuration. Note that the config-

uration of this double bond largely determines the overall molecular shape of this compound class. Accuracy is therefore important if one wants to model the binding mode of this class of compounds to their target proteins correctly.

Because we did not succeed in determining the absolute configuration of this class of compounds through crystal structure determination, we turned to chiral synthesis to solve this problem. Monastrol is a cell-permeable, small-molecule inhibitor of the kinesin Eg5.[27] This molecule is a direct derivative of 4-aryl-3,4-dihydro-2(1*H*)-pyrimidone (DHPMs). The absolute configuration of DHPMs has been well characterized.[28] We realized that monastrol could be used as the starting material for the synthesis of this class of compounds. Thus, monastrol (**1c**) was synthesized through the Biginelli reaction (Scheme 1).[29] The racemic product was then separated by chiral HPLC. Both enantiomers of **1c** (99% *ee*) were dissolved in methanol to obtain their CD spectra and optical rotation values. CD spectra of the first and the second eluted enantiomer are shown in Figure 3. By comparison with the known CD spectra of DHPMs as reference, the enantiomer showing a positive Cotton effect at 303 nm was determined to be the *S* enantiomer, whereas the other was the *R* enantiomer. Measured optical rotation values of (*S*)- and (*R*)-**1c** were +98 and −98 ($c = 1.0$, methanol), respectively.

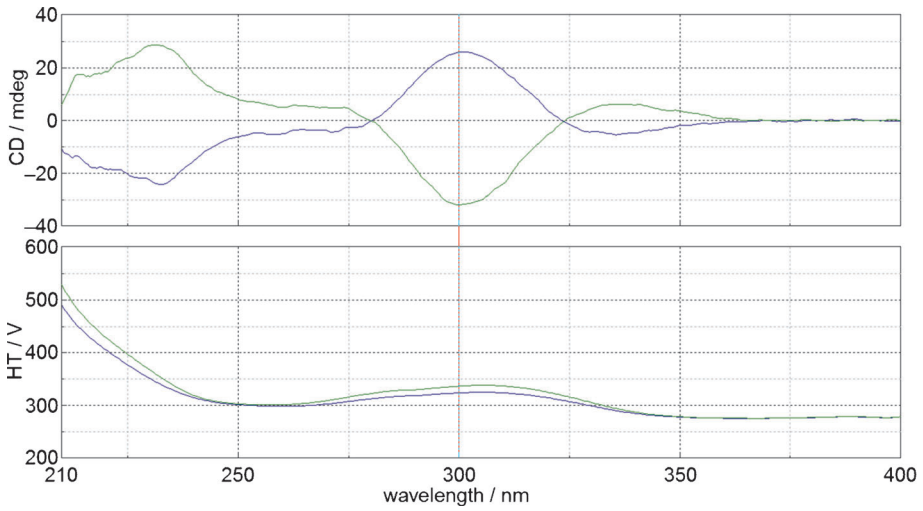

Figure 3. CD spectra of the first and the second eluted enantiomers of **1c** (monastrol). The first eluted enantiomer ((*S*)-**1c**, blue line) exhibited a positive Cotton effect around 303 nm and a negative Cotton effect around 235 and 335 nm, whereas the second enantiomer ((*R*)-**1c**, green line) exhibited a mirror-image pattern.

After optically pure monastrol was obtained, it was then used as the starting material to synthesize two new compounds: **2c** and **2d** (Scheme 1). All obtained enantiomers of **2c**–**d** as well as **2a**–**b** were dissolved in $CHCl_3$ to obtain CD spectra and optical rotation values. The absolute configuration of each enantiomer was determined by examining the pattern observed on its CD spectrum: a positive Cotton effect around 440 nm and a negative effect around 245 nm indicated the *S* enantiomer, whereas the mirror-image pattern indicated the *R* enantiomer. Optical rotation values were also examined as additional proof (see figures S2–S6 in the Supporting Information).

We then selected the two enantiomers of **2a** to examine their binding to Bcl-x_L by CD titration experiments. (*S*)-**2a** and (*R*)-**2a** were tested at six different concentrations up to 50 mM, and the results are shown in Figure 4. In both cases, CD signals were essentially proportional to the concentrations of **2a**, indicating their dose-dependent binding to Bcl-x_L. Although we were unable to derive quantitative association constants within the concentration range tested in this experiment, it is clear that both (*S*)-**2a** and (*R*)-**2a** bind Bcl-x_L with approximately equal binding affinities.

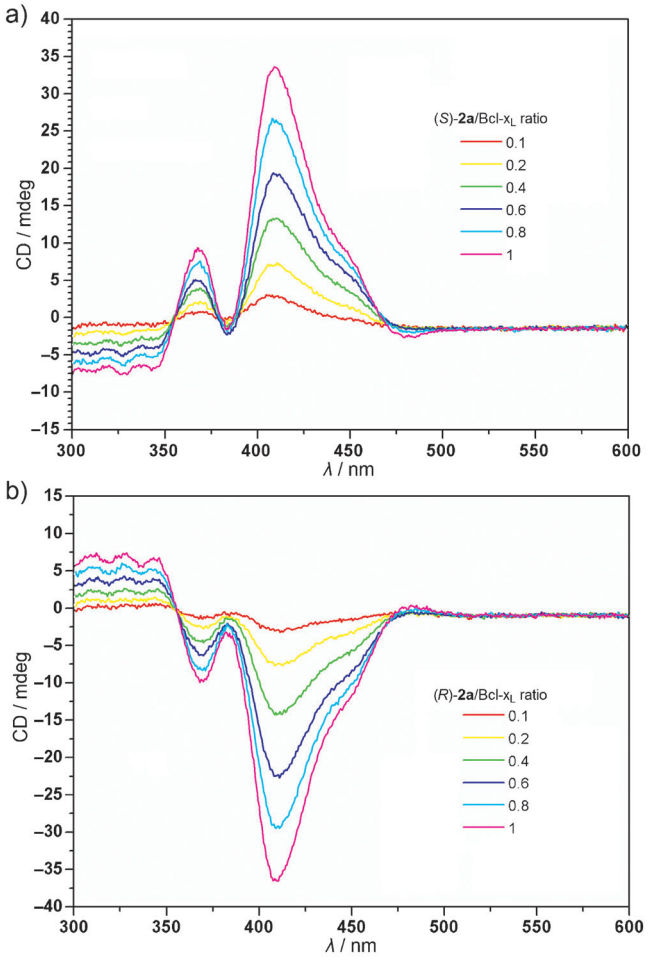

Figure 4. CD spectra of a) (*S*)-**2a** and b) (*R*)-**2a** mixed with Bcl-x_L, which were measured in 5 mM Tris buffer with 5% DMSO; **2a** was tested at six different concentrations up to 50 mM.

To obtain quantitative binding affinities for **2a**–**d** to the three anti-apoptotic Bcl-2 family proteins (Bcl-x_L, Bcl-2, and

Table 1. Binding affinities of the compounds reported in this study for three anti-apoptotic Bcl-2 family proteins.

Compd[a]	Yield [%]	K_i [μM][b]		
		Bcl-x_L	Bcl-2	Mcl-1
(*S*)-**2a**	62	1.10 ± 0.66	0.81 ± 0.30	2.20 ± 0.29
(*R*)-**2a**	62	0.83 ± 0.14	1.10 ± 0.37	0.36 ± 0.24
(*S*)-**2b**	78	0.28 ± 0.04	0.94 ± 0.24	0.32 ± 0.05
(*R*)-**2b**	78	0.55 ± 0.06	1.00 ± 0.11	0.42 ± 0.06
(*S*)-**2c**	85	0.29 ± 0.04	0.56 ± 0.17	0.50 ± 0.12
(*R*)-**2c**	96	0.24 ± 0.06	0.70 ± 0.15	1.20 ± 0.36
(*S*)-**2d**	68	0.34 ± 0.06	0.59 ± 0.25	0.74 ± 0.28
(*R*)-**2d**	74	0.29 ± 0.06	0.54 ± 0.06	0.29 ± 0.10

[a] See Scheme 1 for compound structures. [b] Values are the average ± standard deviation (SD) of three parallel measurements.

Mcl-1), all enantiomers of these compounds were tested in an FP-based in vitro binding assay; the results are summarized in Table 1. Binding affinities of these compounds to three target proteins range by one order of magnitude, that is, 0.24–2.20 μM. Interestingly, in most cases the binding affinity of the *S* enantiomer is similar to that of the corresponding *R* enantiomer on all three proteins, with a maximum difference of twofold. This level of difference is actually close to the intrinsic limit of this type of binding assay. The only exception is observed for **2a** at Mcl-1, for which the binding affinity of the *R* enantiomer (K_i = 0.36 μM) is sixfold higher than that of the *S* enantiomer (K_i = 2.20 μM). However, this discrepancy can be reasonably explained by a predicted binding mode of this compound class, as discussed below.

Our results disagree with those of Feng et al. obtained with a similar set of compounds. They reported that at least in one case, the *R* enantiomer of their compound was a good binder, while the *S* enantiomer was basically inactive.[26] We did not test their compounds in this study because the samples of their compounds were not available to us. The exact reason for the discrepancy between our results and their results is unknown. One possible explanation is that although our compounds and theirs share a common core structure, these two sets of compounds are still somewhat different in other regions (Figure 1). For example, the major hydrophobic region on our compounds and that on the compounds of Feng and colleagues are at opposite ends of the molecular framework. Thus, these two sets of compounds may behave differently in their binding to anti-apoptotic Bcl-2 family proteins.

To seek a reasonable interpretation of our binding assay results, we selected **2b** to examine the binding modes of its *S* and *R* enantiomers with Bcl-x_L and Mcl-1 through molecular modeling. The most stable binding modes of (*S*)-**2b** and (*R*)-**2b** with Mcl-1 predicted by us are shown in Figure 5. The binding modes of these two compounds to Bcl-x_L are given in the Supporting Information.

First of all, a reasonable binding mode was obtained for both (*S*)-**2b** and (*R*)-**2b**, suggesting that both enantiomers are effective binders of Mcl-1. A common feature in these two binding modes is the location of the benzyl indole moiety on **2b** in a hydrophobic cavity formed by residues M231, V249,

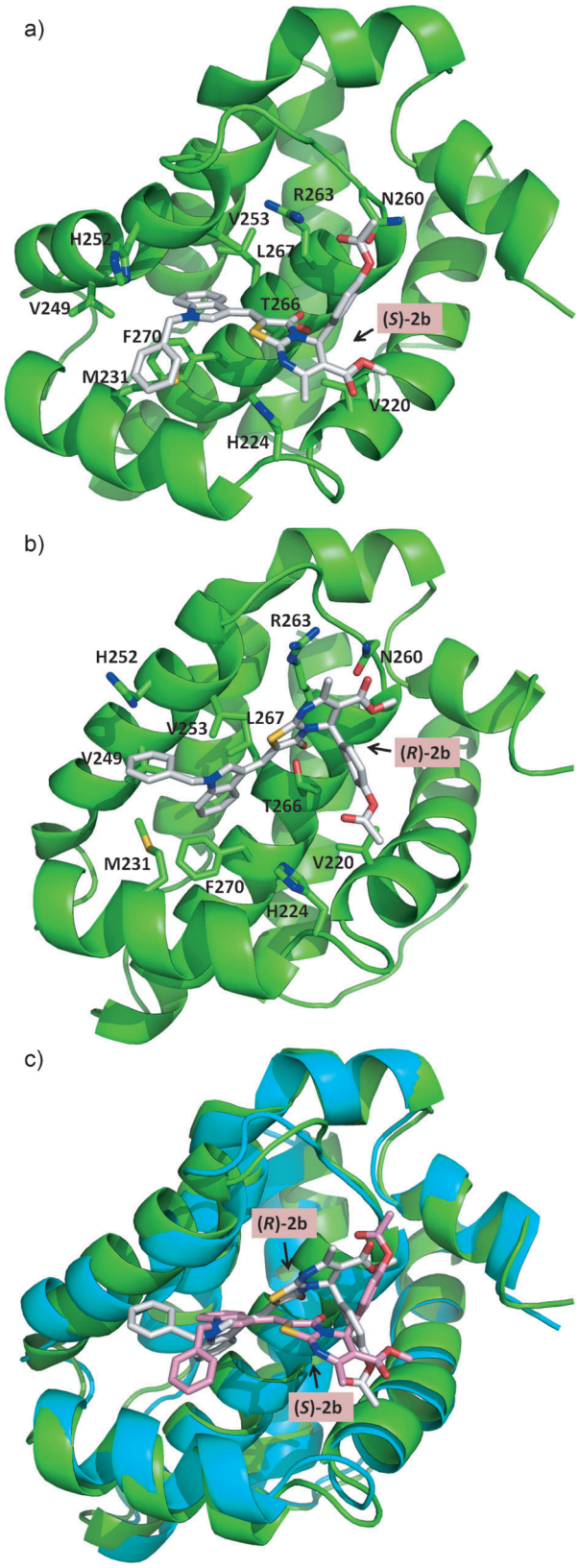

Figure 5. Binding modes of a) (*S*)-**2b** and b) (*R*)-**2b** in complex with Mcl-1 predicted by molecular modeling. Compound **2b** is rendered in stick model, while Mcl-1 is shown as green ribbons. Residues in direct contact with **2b** are shown and labeled explicitly. c) Superimposition of these two complex structures.

V253, L267, and F270. This hydrophobic cavity is common among Bcl-x_L, Bcl-2, and Mcl-1. Such hydrophobic interaction is perhaps the critical factor for binding of **2b** to Bcl-x_L. Indeed, the structure–activity relationships of this compound class, obtained in our previous study, indicate that replacement of this moiety with a phenyl moiety leads to a total loss of binding affinity.[23] This interaction pattern is also observed with other small-molecule Bcl-2 inhibitors such as those in PDB entries 2YXJ,[7] 4EHR,[21] and 4HW2.[22] Moreover, there is a possible hydrogen bond formed between the carbonyl group on the thiazole ring on **2b** and the hydroxy group on the side chain of T266 in both cases. T266 locates approximately at the center of the binding groove on Mcl-1, and this hydrogen bond acts as an anchor for immobilizing (*S*)-**2b** or (*R*)-**2b** during their binding.

Nevertheless, the most apparent difference between the binding modes of (*S*)-**2b** and (*R*)-**2b** lies in the orientation of the substituted phenyl group on the C4 atom, which is a natural consequence of the different configuration of this atom. In the case of (*S*)-**2b**, this substituted phenyl ring points toward N260 and R263 at one side of the binding groove. The acetyl group on it, that is, R^1 in Scheme 1, may form a hydrogen bond with R263. In the case of (*R*)-**2b**, the substituted phenyl ring points toward the other side. Instead, the ester group on C5, that is, R^2 in Scheme 1, may form a hydrogen bond with N260. This part of the binding groove is relatively open, as it is close to the C terminus of Mcl-1, providing enough space for accommodating these two different binding modes. Also, one can see clearly in the superimposed binding modes of (*S*)-**2b** and (*R*)-**2b** that the core structure of **2b** must also adjust its position and orientation in these two cases to allow the substituted phenyl group to stretch into different directions. In particular, as mentioned above, the binding affinity of (*R*)-**2a** to Mcl-1 is sixfold higher than that of (*S*)-**2a**. Note that this compound does not have any substituent on the phenyl ring (Scheme 1). If assuming the binding modes of (*S*)-**2a** and (*R*)-**2a** are similar to the counterparts of **2b**, (*S*)-**2a** cannot form polar interactions with either N260 or R263, whereas (*R*)-**2a** can with the ester group on the C5 atom. Therefore, (*R*)-**2a** is preferred over (*S*)-**2a** in binding to Mcl-1.

To summarize, our predicted binding mode for **2b** illustrates the key role of the benzyl indole moiety as well as the thiazole core moiety in the binding of this class of compounds to Bcl-2 family proteins. However, the substituent groups on C4 and C5, either in the *S* or *R* enantiomer, are not optimal for fitting this part of the binding groove. The hydrogen bonds formed by **2b** with either N260 or R263 were observed to be unstable during molecular dynamics (MD) simulations. This explains the fact that the structure–activity relationships for this class of compounds are less clear when structural modifications are made at these two positions.[23]

It is also interesting to compare the binding mode of our compounds with those reported by Feng et al. For this purpose, we also reproduced the binding mode of Feng's compound **1** to Bcl-x_L as shown in Feng's study.[26] Detailed descriptions can be found in the Supporting Information. Although the predicted binding mode of Feng's compound is actually reasonable, it is not clear from this model why the *R* enantiomer of this compound is a good binder, whereas the *S* enantiomer is basically inactive. Furthermore, the location of the chiral C4 atom inside the binding groove is quite different between our model and Feng's model. It should be emphasized that the purpose of our study is not to overturn the results of Feng et al., but to raise awareness of the disputes on the structure–activity relationships of this class of compounds as Bcl-2 inhibitors. The ultimate answer will be provided by crystal complex structures as well as more careful measurements.

Conclusions

In this study we resolved the stereochemical structures of four 2*H*-thiazolo[3,2-*a*]pyrimidine compounds and investigated their binding affinities toward three anti-apoptotic Bcl-2 family proteins. Interestingly, the *R* and *S* enantiomers of most tested compounds exhibited similar binding affinities for all three proteins. According to our predicted binding mode, the chiral part in the molecular structure of this compound class resides at a relatively open region in the binding site, and the binding site is also sufficiently flexible to accommodate both enantiomers. Therefore, the difference in chirality does not lead to a significant difference in binding affinity for this class of compounds. Notably, our results disagree with those reported by Feng et al. on a similar set of compounds.[26] Readers should be aware of this dispute. The exact binding mode of this class of compounds remains to be resolved by experimental methods. Nevertheless, it is clear, based on the outcomes of this study, that the benzyl indole moiety plays a key role in maintaining the binding affinities of this compound class. On the other hand, the pyrimidine ring along with its substituent groups require further optimization in order to develop this class of compounds into even more promising Bcl-2 inhibitors.

Experimental Section

Compound synthesis: Four compounds (**2a**–**d**) were synthesized as outlined in Scheme 1. Dihydropyrimidine derivatives **1a**–**c** were prepared through the classic Biginelli reaction[29] of commercially available β-keto esters or amides, substituted phenyl aldehydes and thiourea in ethanol at reflux. The reaction was catalyzed by *para*-toluenesulfonic acid monohydrate. Products were then allowed to react with N-substituted 1*H*-indole-3-carbaldehyde and 2-chloroacetic acid in the presence of acetic acid, acetic anhydride, and sodium acetate at 80 °C to obtain **2a**–**d** with yields in the range of 62–96 % (Table 1).

All NMR spectra were recorded at room temperature on a Bruker AV-400 400 MHz spectrometer. They were calibrated using residual undeuterated chloroform ($\delta_H = 7.26$ ppm) and $CDCl_3$ ($\delta_C = 77.16$ ppm) and undeuterated methanol ($\delta_H = 3.31$ ppm), CD_3OD ($\delta_C = 49.00$ ppm) as internal references. The following abbreviations are used to designate multiplicities: s = singlet, d = doublet, t = triplet, q = quartet, m = multiplet, quint = quintet, br = broad. High-resolution mass spectra (HRMS) were recorded on a Bruker APEXIII 7.0 Tesla ESI-FT mass spectrometer at an emitter voltage of 4000 V . Spectral data for compounds **1a**–**1c** and **2a**–**2d** are given below.

6-Methyl-*N*,4-diphenyl-2-thioxo-1,2,3,4-tetrahydropyrimidine-5-carboxamide (1 a): ^{1}H NMR (300 MHz, [D$_6$]DMSO): δ = 10.00 (s, 1 H), 9.74 (s, 1 H), 9.45 (s, 1 H), 7.54 (d, J = 8.1 Hz, 2 H), 7.38–7.33 (m, 2 H), 7.29–7.23 (m, 5 H), 7.02 (d, J = 7.5 Hz, 1 H), 5.40 (d, J = 2.4 Hz, 1 H), 2.07 ppm (s, 3 H).

Methyl-4-(4-hydroxyphenyl)-6-methyl-2-thioxo-1,2,3,4-tetrahydropyrimidine-5-carboxylate (1 b): ^{1}H NMR (300 MHz, [D$_6$]DMSO): δ = 10.03 (s, 1 H), 9.59 (s, 1 H), 9.44 (s, 1 H), 7.00 (d, J = 8.4 Hz, 2 H), 6.71 (d, J = 8.4 Hz, 2 H), 5.06 (d, J = 3.6 Hz, 1 H), 3.54 (s, 3 H), 2.28 ppm (s, 3 H).

Ethyl-4-(3-hydroxyphenyl)-6-methyl-2-thioxo-1,2,3,4-tetrahydropyrimidine-5-carboxylate (1 c, monastrol): ^{1}H NMR (400 MHz, CD$_3$OD): δ = 7.14–7.10 (t, J = 8 Hz, 1 H), 6.77–6.73 (m, 2 H), 6.69–6.67 (m, 1 H), 5.25 (s, 1 H), 4.10–4.08 (q, J = 1.2 Hz, J = 5.6 Hz, 2 H), 2.34 (s, 3 H), 1.20–1.16 ppm (t, J = 7.2 Hz, 3 H); ^{13}C NMR (100 MHz, CD$_3$OD): δ = 175.9, 167.3, 158.7, 146.0, 145.6, 130.6, 118.9, 115.8, 114.5, 103.1, 61.3, 56.3, 17.6, 14.4 ppm; MS (ESI): m/z 293 [M+H]$^+$; HRMS (ESI): m/z calcd for $C_{14}H_{16}N_2O_3SNa^+$ [M+Na]$^+$: 315.0773, obsd: 315.0779; (*S*)-**1 c**, $[\alpha]_D^{25}$: +98 (c = 1.0, MeOH), 99.6 % *ee*, t_R = 5.9 min; (*R*)-**1 c**, $[\alpha]_D^{25}$: −98 (c = 1.0, MeOH), 97.6 % *ee*, t_R = 7.2 min.

(*Z*)-2-((1-Benzyl-1*H*-indol-3-yl)methylene)-7-methyl-3-oxo-*N*,5-diphenyl-3,5-dihydro-2*H*-thiazolo[3,2-*a*]pyrimidine-6-carboxamide (2 a, BCL-LZH-02): ^{1}H NMR (300 MHz, [D$_6$]DMSO): δ = 10.03 (s, 1 H), 8.11 (s, 1 H), 8.03 (s, 1 H), 7.91 (d, J = 7.2 Hz, 1 H), 7.56 (dd, J = 7.8 Hz, 1.5 Hz, 3 H), 7.38–7.17 (m, 14 H), 7.05 (t, J = 7.5 Hz, 1 H), 6.24 (s, 1 H), 5.61 (s, 2 H), 2.13 ppm (d, J = 0.6 Hz, 3 H); ^{13}C NMR (100 MHz, CDCl$_3$): δ = 165.3, 154.8, 143.5, 139.7, 137.5, 136.7, 135.6, 130.3, 129.4, 129.3, 129.2, 129.0, 128.5, 128.1, 127.6, 127.3, 126.8, 124.9, 124.8, 123.9, 122.0, 120.1, 119.1, 113.9, 111.7, 110.6, 56.4, 51.1, 29.8, 21.9 ppm; MS (ESI): m/z 581 [M+H]$^+$; HRMS (ESI): m/z calcd for $C_{36}H_{29}N_4O_2S^+$ [M+H]$^+$: 581.2006, obsd: 581.2015; (*S*)-**2 a**, $[\alpha]_D^{25}$: +851 (c = 0.3, CHCl$_3$), 96.2 % *ee*, t_R = 5.6 min; (*R*)-**2 a**, $[\alpha]_D^{25}$: −730 (c = 0.3, CHCl$_3$), 96.9 % *ee*, t_R = 6.7 min.

(*Z*)-Methyl-5-(4-acetoxyphenyl)-2-((1-benzyl-1*H*-indol-3-yl)methylene)-7-methyl-3-oxo-3,5-dihydro-2*H*-thiazolo[3,2-*a*]pyrimidine-6-carboxylate (2 b, BCL-LZH-18): ^{1}H NMR (300 MHz, CDCl$_3$): δ = 8.09 (s, 1 H), 7.79–7.76 (m, 1 H), 7.46–7.15 (m, 12 H), 7.03 (d, J = 8.4 Hz, 2 H), 6.22 (s, 1 H), 5.37 (s, 2 H), 3.67 (s, 3 H), 2.52 (s, 3 H), 2.26 ppm (s, 3 H); ^{13}C NMR (100 MHz, CDCl$_3$): δ = 169.2, 166.0, 165.1, 156.7, 153.4, 150.6, 137.8, 136.5, 135.4, 130.3, 129.0, 128.9, 128.3, 127.9, 127.1, 126.6, 125.4, 123.8, 121.9, 121.6, 118.9, 113.7, 111.4, 110.4, 107.9, 54.4, 51.5, 50.9, 22.9, 21.1 ppm; MS (ESI): m/z 578 [M+H]$^+$, 600 [M+Na]$^+$; HRMS (ESI): m/z calcd for $C_{33}H_{28}N_3O_5S^+$ [M+H]$^+$: 578.1744, obsd: 578.1751; (*S*)-**2 b**, $[\alpha]_D^{25}$: +706 (c = 0.3, CHCl$_3$), 98.0 % *ee*, t_R = 4.2 min; (*R*)-**2 b**, $[\alpha]_D^{25}$: −982 (c = 0.3, CHCl$_3$), 98.0 % *ee*, t_R = 4.6 min.

(*Z*)-Methyl-2-((1-benzyl-1*H*-indol-3-yl)methylene)-5-(4-hydroxyphenyl)-7-methyl-3-oxo-3,5-dihydro-2*H*-thiazolo[3,2-*a*]pyrimidine-6-carboxylate (deacetylated 2 b, BCL-LZH-18A): ^{1}H NMR (400 MHz, CDCl$_3$): δ = 8.11 (s, 1 H), 7.77–7.75 (m, 1 H), 7.42 (s, 1 H), 7.32–7.24 (m, 8 H), 7.15–7.13 (d, 2 H), 6.74–6.72 (d, 2 H), 6.17 (s, 1 H), 5.36 (s, 2 H), 3.66 (s, 3 H), 2.52 ppm (s, 3 H); MS (ESI): m/z 536 [M+H]$^+$; HRMS (ESI): m/z calcd for $C_{31}H_{26}N_3O_4S^+$ [M+H]$^+$: 536.1649, obsd: 536.1638.

(*Z*)-Ethyl-5-(3-acetoxyphenyl)-2-((1-benzyl-1*H*-indol-3-yl)methylene)-7-methyl-3-oxo-3,5-dihydro-2*H*-thiazolo[3,2-*a*]pyrimidine-6-carboxylate (2 c, BCL-LZH-11A): ^{1}H NMR (400 MHz, CDCl$_3$): δ = 8.10 (s, 1 H), 7.80–7.78 (m, 1 H), 7.39 (s, 1 H), 7.34–7.17 (m, 8 H), 7.17–7.15 (m, 3 H), 7.03–7.02 (m, 1 H), 6.21 (s, 1 H), 5.37 (s, 2 H), 4.12–4.10 (q, J = 1.2 Hz, J = 5.6 Hz, 2 H), 2.52 (s, 3 H), 2.27 (s, 3 H), 1.21–1.17 ppm (t, J = 7.2 Hz, 3 H); ^{13}C NMR (100 MHz, CDCl$_3$): δ = 169.1, 165.4, 165.1, 156.6, 153.2, 150.7, 141.9, 136.5, 135.5, 130.3, 129.5, 129.1, 128.3, 128.0, 127.2, 125.4, 123.8, 121.9, 121.2, 119.0, 113.6, 111.5, 110.5, 108.0, 60.55, 54.8, 50.9, 22.9, 21.2, 14.0 ppm; MS (ESI): m/z 592 [M+H]$^+$; HRMS (ESI): m/z calcd for $C_{34}H_{30}N_3O_5S^+$ [M+H]$^+$: 592.1900, obsd: 592.1891; (*S*)-**2 c**, $[\alpha]_D^{25}$: +1033 (c = 0.3, CHCl$_3$), 99.5 % *ee*, t_R = 17.8 min; (*R*)-**2 c**, $[\alpha]_D^{25}$: −1000 (c = 0.3, CHCl$_3$), 98.9 % *ee*, t_R = 23.5 min.

(*Z*)-Ethyl-2-((1-([1,1′-biphenyl]-4-ylmethyl)-1*H*-indol-3-yl)methylene)-5-(3-acetoxyphenyl)-7-methyl-3-oxo-3,5-dihydro-2*H*-thiazolo[3,2-*a*]pyrimidine-6-carboxylate (2 d, BCL-LZH-42A): ^{1}H NMR (400 MHz, CDCl$_3$): δ = 8.08 (s, 1 H), 7.80–7.79 (m, 1 H), 7.56–7.54 (m, 4 H), 7.45–7.41 (m, 3 H), 7.37–7.28 (m, 6 H), 7.26–7.21 (m, 2 H), 7.16 (s, 1 H), 7.03–7.02 (m, 1 H), 6.21 (s, 1 H), 5.42 (s, 2 H), 4.12–4.10 (q, J = 1.2 Hz, J = 5.6 Hz, 2 H), 2.52 (s, 3 H), 2.26 (s, 3 H), 1.21–1.17 ppm (t, J = 7.2 Hz, 3 H); ^{13}C NMR (100 MHz, CDCl$_3$): δ = 169.1, 165.4, 165.1, 156.6, 153.2, 150.7, 141.9, 136.5, 135.5, 130.3, 129.4, 129.1, 128.8, 128.3, 1282.0, 127.2, 125.5, 125.4, 123.8, 121.9, 121.2, 118.9, 113.6, 111.4, 110.5, 108.0, 60.5, 54.8, 50.9, 22.9, 21.2, 14.0 ppm; MS (ESI): m/z 668 [M+H]$^+$; HRMS (ESI): m/z calcd for $C_{40}H_{34}N_3O_5S^+$ [M+H]$^+$: 668.2213, obsd: 668.2210; (*S*)-**2 d**, $[\alpha]_D^{25}$: +691 (c = 0.3, CHCl$_3$), 99.7 % *ee*, t_R = 54.7 min; (*R*)-**2 d**, $[\alpha]_D^{25}$: −703 (c = 0.3, CHCl$_3$), 98.7 % *ee*, t_R = 86.3 min.

HPLC and CD spectra: Chiral HPLC separation of **2 a** and **2 b** was performed at 35 °C using a chromatography system consisting of a CHIRALPAK IA column (46 mm × 250 mm, 10 μm) and a Shimadzu LC 20 instrument equipped with an SPD-20A UV detector; detection was at λ 254 nm and the flow rate was 1.0 mL min^{-1}. MeOH/CH$_2$Cl$_2$ 95:5 and CH$_2$Cl$_2$/CH$_3$CN 95:5 mixtures (*v*/*v*) were used as the eluting solvent for **2 a** and **2 b**, respectively. Retention times for (*S*)-**2 a** and (*R*)-**2 a** were 5.6 and 6.7 min, respectively. Retention times for (*S*)-**2 b** and (*R*)-**2 b** were 4.2 and 4.6 min, respectively. The racemic mixture of **1 c** was separated by using a Chiralcel OJ-H column (i.d. = 0.46 cm × l = 25 cm; mobile phase: hexane/EtOH = 70:30 *v*/*v*; T = 35 °C). Retention times for (*S*)-**1 c** and (*R*)-**1 c** were 5.9 and 7.2 min, respectively.

All CD spectra were obtained with a Jasco J-810 spectropolarimeter using standard conditions. Sample solutions in methanol were placed in quartz cells of 10 mm path length, and their concentrations were adjusted to 0.05 mg mL^{-1}. Sample solutions were prepared at room temperature. CD spectra were taken with the following settings: scan rate = 500 nm min^{-1}; bond width = 0.1 nm; response time = 1.0 s; accumulations = 2 scan. Optical rotations were measured in a 10 mm quartz cell on a Jasco P-1030 polarimeter. HPLC and CD spectra and optical rotation values of compounds **1 c, 2 a**–**d** are given in the Supporting Information.

CD titration was performed for (*R*)-**2 a** and (*S*)-**2 a** binding to Bcl-x$_L$. The concentration of Bcl-x$_L$ used in this experiment was 50 mM. Six different concentrations of **2 a** (5, 10, 20, 30, 40, and 50 mM) were tested in 5 mM Tris buffer (pH 7.5) with 5 % DMSO. CD signals were recorded between 300 and 600 nm on a Jasco J-715 spectropolarimeter at room temperature in a cuvette of 1 cm path length. All spectra were accumulated twice at a bandwidth of 1.0 nm and a resolution of 0.5 nm at a scan speed of 100 nm min^{-1}. This experiment was not performed for other compounds reported in this study, because it consumed too much protein sample on the spectropolarimeter accessible to us and yet was difficult to derive quantitative binding data.

Crystal structure determination: Growth of single crystals was attempted for the *R* and *S* enantiomers of **2 a** and **2 b** as well as their racemic mixture. These attempts, however, failed to obtain single

crystals good enough for structure determination. Nevertheless, good crystals were obtained from the racemic mixture of deacetylated **2b** with the following methods: The compound sample (15 mg) and THF (2.0 mL) were added to a 5 mL sample bottle. The sample bottle was then transferred into a 60 mL reagent bottle containing 20 mL petroleum ether. The solution was allowed to stand for several days to obtain the final crystals.

X-ray crystal diffraction data were collected on a Bruker Apex II CCD diffractometer operating at 50 kV and 30 mA using $Mo_{K\alpha}$ radiation ($\lambda = 0.71073$ Å) at 133 K. Main features of this crystal structure are: $C_{39}H_{41}N_3O_6S$, $M_r = 679.81\ g\,mol^{-1}$, crystal size $0.35 \times 0.10 \times 0.05$ mm, triclinic, space group = $P1$, $a = 9.4103(13)$ Å, $b = 11.5966(16)$ Å, $c = 15.993(2)$ Å, $\alpha = 79.623(2)^\circ$, $\beta = 85.822(2)^\circ$, $\gamma = 78.788(2)^\circ$, $V = 1682.6(4)$ Å^3, $T = 133$ K, $Z = 2$, $D_{calc} = 1.342\ g\,cm^{-3}$, $\lambda = 0.71073$ Å, $\mu(Mo_{K\alpha}) = 8.396\ mm^{-1}$. Other details are given in the Supporting Information. In addition, CCDC 942185 contains the supplementary crystallographic data for this paper. These data can be obtained free of charge from The Cambridge Crystallographic Data Centre via www.ccdc.cam.ac.uk/data_request/cif.

In vitro binding assays: A fluorescence polarization (FP)-based assay was employed in this study to measure the binding affinities of small-molecule compounds to three anti-apoptotic Bcl-2 family proteins: Bcl-x_L, Bcl-2, and Mcl-1. Competitive binding of a given compound was characterized quantitatively by monitoring the changes in FP signal upon addition of test compound at multiple concentrations.

The Bcl-x_L protein used in our study is a special truncated construction of the full-length protein, with deletion of residues 45–84 on a large loop region and residues 210–233 at the C-terminal hydrophobic region. The Bcl-2 protein used in our study has the same construction as that (Bcl-2/Bcl-x_L, isoform 2) reported by Fesik et al.,[30] which is composed of residues 1–34 of human Bcl-2, residues 29–44 of human Bcl-x_L, and residues 92–207 of human Bcl-2. The Mcl-1 protein used in our study has the same construction as that (hMcl-1BLR) used in the work of Colman et al.,[31] which is composed of residues 152–189 of mouse Mcl-1 and residues 209–327 of human Mcl-1. Methods used for preparing the samples of these three proteins are given in the Supporting Information.

A 26-residue peptide derived from the BH3 domain of the Bid protein with 5-carboxyfluorescein (5-FAM) on the N terminus, that is, 5-(FAM)-QEDIIRNIARHLAQVGDSMDRSIPPG, was used as the fluorescence tracer (HD Biosciences). The desired sequence was verified by amino acid component analysis and MS. The purity of this peptide was >95%, as verified by HPLC. Our dose-dependent saturation experiments determined that this Bid-BH3 peptide binds to Bcl-x_L with $K_d = 41$ nM, to Bcl-2 with $K_d = 89$ nM, and to Mcl-1 with $K_d = 29$ nM (see figure S7 in the Supporting Information).

In competitive binding measurements, each protein (Bcl-x_L, Bcl-2, or Mcl-1) and the compound under test (in 1% [D_6]DMSO solution) were pre-incubated in the assay buffer (PBS, pH 7.3, 140 mM NaCl, 2.7 mM KCl, 10 mM Na_2HPO_4, 1.8 mM KH_2PO_4) at 37 °C for 30 min. A solution in PBS of the FAM-Bid peptide (20 μL) was then added to the solution to produce a final volume of 200 μL and incubated at 37 °C for another 20 min. The total concentration of the Bid-BH3 peptide used in assay was 10 nM, while the total concentration of protein was set to fivefold the K_d value of the fluorescence tracer. Finally, the solutions were transferred into black flat-bottomed 384-well plates (Corning Inc.) with 60 μL per well and three wells per sample. Polarization signals (in milipolarization units, mP) were measured at an excitation wavelength of 485 nm and an emission wavelength of 535 nm on a Tecan Genios Pro Injector Reader (Tecan Group Ltd.). In each experiment, a positive control containing the protein (Bcl-x_L, Bcl-2, or Mcl-1), the Bid-BH3 peptide, and 1% (*v*/*v*) [D_6]DMSO, as well as a negative control containing only Bid-BH3 peptide, were included on each plate.

Each compound was tested against all three proteins (Bcl-x_L, Bcl-2, and Mcl-1) at seven different concentrations: 1, 10 and 100 nM, and 1, 10, 50, and 100 μM. At each concentration, the average FP value of three parallel measurements was used to perform nonlinear fitting to obtain the final binding curve. The nonlinear fitting was conducted with GraphPad Prism software (version 5). Concentration of the given compound at which 50% of the bound peptide was displaced (IC_{50}) was derived from the binding curve. The competitive inhibition constant (K_i) of each tested compound was then calculated with an equation developed by Wang et al.[32] assuming formation of a binary complex with the target protein.

Molecular modeling: The binding modes of (*S*)-**2b** and (*R*)-**2b** were predicted through molecular docking and MD simulations. Bcl-x_L and Mcl-1 were considered for this purpose. As the first step, molecular docking was employed to derive a rough binding mode for **2b** with Bcl-x_L and Mcl-1. The complex structure between human Bcl-x_L and the Bak-BH3 peptide (PDB entry: 1BXL) was used in molecular docking of **2b**. For the Mcl-1 protein, the structure from the complex between human Mcl-1 and the Bim-BH3 peptide (PDB entry: 2PQK) was selected for molecular docking. The molecular structures of (*R*)-**2b** and (*S*)-**2b** were sketched with SYBYL software (version 8.1) and optimized with the MMFF94 force field. Automatic docking of each molecule to Bcl-x_L or Mcl-1 was performed by using GOLD software (version 5.1, Cambridge Crystallographic Data Centre). Detailed parameters and settings used in this task are given in the Supporting Information. A total of 30 final binding poses were generated for each ligand molecule. These binding poses were clustered by RMSD values with a cutoff of 2.0 Å. The binding pose with the highest binding score from the largest cluster was selected as the most reasonable one after visual examination.

The selected binding pose of the given compound was then refined through MD simulation using the AMBER program (version 12, University of California San Francisco). Each MD simulation was performed in an explicit water box for 5 ns. Detailed parameters and settings used in our MD simulations are given in the Supporting Information. On each MD trajectory, 5000 snapshots were retrieved at 1 ps intervals. These snapshots were grouped into clusters based on mass-weighted RMSD values with a cutoff value of 1.5 Å. The snapshot closest to the cluster center in the largest cluster was selected as the representative binding mode. The final selected binding modes of (*R*)-**2b** and (*S*)-**2b** to Bcl-x_L and Mcl-1 are shown in figures S10 and S11 in the Supporting Information.

Acknowledgements

The authors are grateful for financial support from the Chinese National Natural Science Foundation (Grant Nos. 81172984, 21072213, 21002117, 21102168, 21102165, and 20921091) and the 863 High-Tech program (Grant No. 2012AA020308) from the Chinese Ministry of Science and Technology.

Keywords: Bcl-2 · binding affinity · chirality · inhibitors · protein–protein interactions · small molecules

[1] J. C. Reed, *Nat. Rev. Drug Discovery* **2002**, *1*, 111 – 121.
[2] S. W. Fesik, *Nat. Rev. Cancer* **2005**, *5*, 876 – 885.
[3] M. H. Andersen, J. C. Becker, P. Straten, *Nat. Rev. Drug Discovery* **2005**, *4*, 399 – 409.
[4] S. Pattingre, A. Tassa, X. P. Qu, R. Garuti, X. H. Liang, N. Mizushima, M. Packer, M. D. Schneider, B. Levine, *Cell* **2005**, *122*, 927 – 939.
[5] Y. M. Janumyan, C. G. Sansam, A. Chattopadhyay, N. L. Cheng, E. L. Soucie, L. Z. Penn, D. Andrews, C. M. Knudson, E. Yang, *EMBO J.* **2003**, *22*, 5459 – 5470.
[6] G. Lessene, P. E. Czabotar, P. M. Colman, *Nat. Rev. Drug Discovery* **2008**, *7*, 989 – 1000.
[7] T. Oltersdorf, S. W. Elmore, A. R. Shoemaker, R. C. Armstrong, D. J. Augeri, B. A. Belli, M. Bruncko, T. L. Deckwerth, J. Dinges, P. J. Hajduk, M. K. Joseph, S. Kitada, S. J. Korsmeyer, A. R. Kunzer, A. Letai, C. Li, M. J. Mitten, D. G. Nettesheim, S. Ng, P. M. Nimmer, J. M. O'Connor, A. Oleksijew, A. M. Petros, J. C. Reed, W. Shen, S. K. Tahir, C. B. Thompson, K. J. Tomaselli, B. Wang, M. D. Wendt, H. Zhang, S. W. Fesik, S. H. Rosenberg, *Nature* **2005**, *435*, 677 – 681.
[8] C. Tse, A. R. Shoemaker, J. Adickes, M. G. Anderson, J. Chen, S. Jin, E. F. Johnson, K. C. Marsh, M. J. Mitten, P. Nimmer, L. Roberts, S. K. Tahir, Y. Xiao, X. Yang, H. Zhang, S. Fesik, S. H. Rosenberg, S. W. Elmore, *Cancer Res.* **2008**, *68*, 3421 – 3428.
[9] S. Kitada, M. Leone, S. Sareth, D. Zhai, J. C. Reed, M. Pellecchia, *J. Med. Chem.* **2003**, *46*, 4259 – 4264.
[10] B. Becattini, S. Kitada, M. Leone, E. Monosov, S. Chandler, D. Zhai, T. J. Kipps, J. C. Reed, M. Pellecchia, *Chem. Biol.* **2004**, *11*, 389 – 395.
[11] M. Nguyen, R. C. Marcellus, A. Roulston, M. Watson, L. Serfass, S. R. M. Madiraju, D. Goulet, J. Viallet, L. Belec, X. Billot, S. Acoca, E. Purisima, A. Wiegmans, L. Cluse, R. W. Johnstone, P. Beauparlant, G. C. Shore, *Proc. Natl. Acad. Sci. USA* **2007**, *104*, 19512 – 19517.
[12] J. L. Wang, D. Liu, Z.-J. Zhang, S. Shan, X. Han, S. M. Srinivasula, C. M. Croce, E. S. Alnemri, Z. Huang, *Proc. Natl. Acad. Sci. USA* **2000**, *97*, 7124 – 7129.
[13] G. Wang, N.-C. Zaneta, C.-Y. Yang, R. Wang, G. Tang, J. Guo, S. Shangary, S. Qiu, W. Gao, D. Yang, J. Meagher, J. Stuckey, K. Krajewski, S. Jiang, P. P. Roller, H. O. Abaan, Y. Tomita, S. Wang, *J. Med. Chem.* **2006**, *49*, 6139 – 6142.
[14] G. Tang, Z. Nikolovska-Coleska, S. Qiu, C.-Y. Yang, J. Guo, S. Wang, *J. Med. Chem.* **2008**, *51*, 717 – 720.
[15] J. Wei, S. Kitada, M. F. Rega, J. L. Stebbins, D. Zhai, J. Cellitti, H. Yuan, A. Emdadi, R. Dahl, Z. Zhang, L. Yang, J. C. Reed, M. Pellecchia, *J. Med. Chem.* **2009**, *52*, 4511 – 4523.
[16] J. Wei, J. L. Stebbins, S. Kitada, R. Dash, W. Placzek, M. F. Rega, B. Wu, J. Cellitti, D. Zhai, L. Yang, R. Dahl, P. B. Fisher, J. C. Reed, M. Pellecchia, *J. Med. Chem.* **2010**, *53*, 4166 – 4176.
[17] Z. Zhang, G. Wu, F. Xie, T. Song, X. Chang, *J. Med. Chem.* **2011**, *54*, 1101 – 1105.
[18] B. E. Sleebs, P. E. Czabotar, W. J. Fairbrother, W. D. Fairlie, J. A. Flygare, D. Huang, W. J. A. Kersten, M. F. T. Koehler, G. Lessene, K. Lowes, J. P. Parisot, B. J. Smith, M. L. Smith, A. J. Souers, I. P. Street, H. Yang, J. B. Baell, *J. Med. Chem.* **2011**, *54*, 1914 – 1926.
[19] J. Chen, H. Zhou, A. Aguilar, L. Liu, L. Bai, D. McEachern, C.-Y. Yang, J. L. Meagher, J. A. Stuckey, S. Wang, *J. Med. Chem.* **2012**, *55*, 8502 – 8514.
[20] H. Zhou, A. Aguilar, J. Chen, L. Bai, L. Liu, J. L. Meagher, C.-Y. Yang, D. McEachern, X. Cong, J. A. Stuckey, S. Wang, *J. Med. Chem.* **2012**, *55*, 6149 – 6161.
[21] G. M. Schroedera, D. Weia, P. Banfib, Z.-W. Caia, J. Lippya, M. Menichincherib, M. Modugnob, J. Naglicha, B. Penhallowa, H. L. Pereza, J. Sacka, R. J. Schmidta, A. Tebbena, C. Yana, L. Zhang, A. Galvanib, L. J. Lombardoa, R. M. Borzilleria, *Bioorg. Med. Chem. Lett.* **2012**, *22*, 3951 – 3956.
[22] A. Friberg, D. Vigil, B. Zhao, R. N. Daniels, J. P. Burke, P. M. Garcia-Barrantes, D. Camper, B. A. Chauder, T. Lee, E. T. Olejniczak, S. W. Fesik, *J. Med. Chem.* **2013**, *56*, 15 – 30.
[23] B. Zhou, X. Li, Y. Li, Y. Xu, Z. Zhang, M. Zhou, X. Zhang, Z. Liu, J. Zhou, C. Cao, B. Yu, R. Wang, *ChemMedChem* **2011**, *6*, 904 – 921.
[24] I. E. Wertz, S. Kusam, C. Lam, T. Okamoto, W. Sandoval, D. J. Anderson, E. Helgason, J. A. Ernst, M. Eby, J. Liu, L. D. Belmont, J. S. Kaminker, K. M. O'Rourke, K. Pujara, P. B. Kohli, A. R. Johnson, M. L. Chiu, J. R. Lill, P. K. Jackson, W. J. Fairbrother, S. Seshagiri, M. J. C. Ludlam, K. G. Leong, E. C. Dueber, H. Maecker, D. C. S. Huang, V. M. Dixit, *Nature* **2011**, *471*, 110 – 114.
[25] S.-H. Wei, K. Dong, F. Lin, X. Wang, B. Li, J.-J. Shen, Q. Zhang, R. Wang, H.-Z. Zhang, *Cancer Chemother. Pharmacol.* **2008**, *62*, 1055 – 1064.
[26] Y. Feng, X. Ding, T. Chen, L. Chen, F. Liu, X. Jia, X. Luo, X. Shen, K. Chen, H. Jiang, H. Wang, H. Liu, D. Liu, *J. Med. Chem.* **2010**, *53*, 3465 – 3479.
[27] T. U. Mayer, T. M. Kapoor, S. J. Haggarty, R. W. King, S. L. Schreiber, T. J. Mitchison, *Science* **1999**, *286*, 971 – 974.
[28] W. Krenn, P. Verdino, G. Uray, K. Faber, C. O. Kappe, *Chirality* **1999**, *11*, 659 – 662.
[29] T. S. Jin, S. L. Zhang, T. S. Li, *Synth. Commun.* **2002**, *32*, 1847 – 1851.
[30] A. M. Petros, A. Medek, D. G. Nettesheim, D. H. Kim, H. S. Yoon, K. Swift, E. D. Matayoshi, T. Oltersdorf, S. W. Fesik, *Proc. Natl. Acad. Sci. USA* **2001**, *98*, 3012 – 3017.
[31] P. E. Czabotar, E. F. Lee, M. F. van Delft, C. L. Day, B. J. Smith, D. C. Huang, W. D. Fairlie, M. G. Hinds, P. M. Colman, *Proc. Natl. Acad. Sci. USA* **2007**, *104*, 6217 – 6222.
[32] Z. Nikolovska-Coleska, R. Wang, X. Fang, H. Pan, Y. Tomita, P. Li, P. P. Roller, K. Krajewski, N. G. Saito, J. A. Stuckey, S. Wang, *Anal. Biochem.* **2004**, *332*, 261 – 273.

Received: April 11, 2013
Revised: May 31, 2013
Published online on ■■ ■■, 0000